

CONFIDENTIAL

N 62 59259

CLASSIFICATION  
CHANGED TO RESTRICTED



# RESEARCH MEMORANDUM

CLASSIFICATION CHANGED TO  
UNCLASSIFIED

AUTHORITY CROWLEY CHANGE #2104

DATE 12-14-53

T.C.F.

AERODYNAMIC CHARACTERISTICS OF A 45° SWEEP-BACK WING

WITH ASPECT RATIO OF 3.5 AND NACA 2S-50(05) -50(05)

AIRFOIL SECTIONS

By

Anthony J. Proterra

Langley Memorial Aeronautical Laboratory  
Langley Field, Va.

CLASSIFIED DOCUMENT

This document contains classified information affecting the National Defense of the United States within the meaning of the Espionage Act, USC 50:31 and 32. Its transmission or the revelation of its contents in any manner to an unauthorized person is prohibited by law. Information so classified may be imparted only to persons in the military and naval services of the United States, appropriate civilian officers and employees of the Federal Government who have a legitimate interest therein, and to United States citizens of known loyalty and discretion who of necessity must be informed thereof.

## NATIONAL ADVISORY COMMITTEE FOR AERONAUTICS

WASHINGTON

August 4, 1947

CONFIDENTIAL

CLASSIFICATION

CHANGED TO RESTRICTED

CONFIDENTIAL

E R R A T U M

NACA RM No. L7C11

AERODYNAMIC CHARACTERISTICS OF A  $45^\circ$  SWEEP-BACK WING WITH ASPECT  
RATIO OF 3.5 AND NACA 2S-50(05)-50(05) AIRFOIL SECTIONS

By Anthony J. Proterra

August 4, 1947

The last sentence of the first paragraph of the section entitled "DISCUSSION OF FLOW PHENOMENA" (p. 7) has been found to be in error. Lines 15-17 of this paragraph should read as follows:

"fashion; whereas, a conventional section is characterized by an initial separation which occurs at a much higher angle of attack and further aft on the airfoil surface."

CONFIDENTIAL

## NATIONAL ADVISORY COMMITTEE FOR AERONAUTICS

## RESEARCH MEMORANDUM

AERODYNAMIC CHARACTERISTICS OF A  $45^\circ$  SWEEP-BACK WING

WITH ASPECT RATIO OF 3.5 AND NACA 2S-50(05)-50(05)

## AIRFOIL SECTIONS

By Anthony J. Proterra

## SUMMARY

The results of an investigation to determine the aerodynamic characteristics at high Reynolds numbers and low Mach numbers of a  $45^\circ$  swept-back wing with aspect ratio 3.5, taper ratio of 0.5 and circular-arc sections are presented in this report. Scale effects were investigated at Reynolds numbers ranging from  $2.1 \times 10^6$  to  $8.0 \times 10^6$ ; the effects of yaw were investigated at a Reynolds number of  $4.1 \times 10^6$ .

The results indicate that the wing has poor characteristics from low-speed considerations. The wing has a maximum lift coefficient of approximately 0.87 and has high drag at high angles of attack. The longitudinal stability is neutral up to a lift coefficient of approximately 0.3 and increases above this value to a lift coefficient of approximately 0.5. Between a lift coefficient of 0.5 and maximum lift coefficient  $C_{L_{max}}$  the wing is longitudinally unstable but at  $C_{L_{max}}$  the wing has a diving tendency. The effective dihedral is positive up to a lift coefficient of 0.45 but is negative above this value. The wing has neutral directional stability up to a lift coefficient of 0.45 and is directionally unstable at higher lift coefficients. The lift, drag, and pitching-moment coefficients are almost unaffected by variations in Reynolds number.

## INTRODUCTION

The proposed use of swept and low-aspect-ratio wing plan forms and biconvex profiles to minimize compressibility effects at transonic and supersonic speeds has emphasized the need for data on the full-scale aerodynamic characteristics of these wings at low Mach numbers.

A study is, therefore, being made in the Langley full-scale tunnel of the low-speed characteristics of wings having 10-percent-thick circular-arc supersonic airfoils and various high-lift devices. As a part of this study an investigation has been made with a  $45^\circ$  swept-back wing of aspect ratio 3.5 and taper ratio 0.5.

The present paper presents the scale effect on the longitudinal aerodynamic characteristics, the aerodynamic characteristics in yaw, and the tuft studies for  $0^\circ$  and  $3.7^\circ$  yaw. The results of the effect of leading-edge and trailing-edge flaps on the aerodynamic characteristics of the wing will be presented in later reports.

### COEFFICIENTS AND SYMBOLS

The data are referred to the stability axes, which are a system of axes in which the Z-axis is in the plane of symmetry and perpendicular to the relative wind, the X-axis is in the plane of symmetry and perpendicular to the Z-axis, and the Y-axis is perpendicular to the plane of symmetry. The origin was located at quarter chord of mean aerodynamic chord. The positive directions of forces, of moments, of angular displacements of the model are given in figure 1.

$C_L$  lift coefficient  $\left(\frac{\text{Lift}}{qS}\right)$

$C_X$  longitudinal-force coefficient  $\left(\frac{X}{qS}\right)$

$C_Y$  lateral-force coefficient  $\left(\frac{Y}{qS}\right)$

$C_m$  pitching-moment coefficient  $\left(\frac{M}{qSc}\right)$

$C_n$  yawing-moment coefficient  $\left(\frac{N}{qSb}\right)$

$C_l$  rolling-moment coefficient  $\left(\frac{L}{qSb}\right)$

X longitudinal force, pounds

Y lateral force, pounds

M pitching moment about the  $\frac{\bar{c}}{4}$ , foot-pounds; positive when the moment tends to increase angle of attack

- N yawing moment about the  $\frac{\bar{c}}{4}$ , foot-pounds; positive when the moment tends to retard the right wind panel
- L rolling moment about the  $\frac{\bar{c}}{4}$ , foot-pounds; positive when the moment tends to raise the left wing panel
- $C_{l\psi}$  rate of change of rolling-moment coefficient with angle of yaw,  $\frac{dC_l}{d\psi}$ , per degree
- $C_{n\psi}$  rate of change of yawing-moment coefficient with angle of yaw,  $\frac{dC_n}{d\psi}$ , per degree
- $C_{y\psi}$  rate of change of lateral-force coefficient with angle of yaw,  $\frac{dC_y}{d\psi}$ , per degree
- q free-stream dynamic pressure  $\left(\frac{1}{2}\rho V^2\right)$
- V free-stream velocity, feet per second
- S wing area (231 sq ft)
- b wing span (28.5 ft)
- $\bar{c}$  mean aerodynamic chord measured parallel to plane of symmetry (8.37 ft)
- $\bar{x}$  distance from leading edge of root chord to quarter chord of the mean aerodynamic chord (9.03 ft)
- R Reynolds number  $\left(\frac{V\bar{c}}{\gamma}\right)$
- $\alpha$  angle of attack measured in plane of symmetry, degrees
- $\psi$  angle of yaw, positive when right wing panel is retarded, degrees
- $\gamma$  kinematic viscosity, square feet per second

## MODEL

The plan form of the wing is given in figure 2. A general view of the wing mounted on full-scale tunnel balance supports is

shown in figure 3. The wing has an angle of sweep of  $45^\circ$  at the quarter-chord line. The airfoil sections perpendicular to the 50-percent chord line are circular-arc sections and have a maximum thickness of 10 percent at the 50-percent chord. The model has an aspect ratio of 3.5 and a taper ratio of 0.5 with the wing tips slightly rounded. The wing has no geometric dihedral or twist.

The wing was constructed of 1/4-inch aluminum sheet reinforced by steel channel spars. The wing surfaces were about the equivalent in roughness to conventional thin dural sheet construction with dimpled skin and unfilled flush rivets. The wing construction was extremely rigid and it is not believed that deflections of any appreciable magnitude occurred during the tests.

#### TEST PROCEDURE

All tests were made through an angle-of-attack range from  $-1^\circ$  to  $28^\circ$  and readings were taken at increments of  $2^\circ$  angle of attack except near maximum lift where increments of  $1^\circ$  were used.

In order to determine the scale effect on the aerodynamic characteristics at  $0^\circ$  yaw the wing was tested through a Reynolds number range of  $2.1 \times 10^6$  to  $8.0 \times 10^6$ . This was accomplished by varying the tunnel speed.

The wing was tested through the angle-of-yaw range from  $-6^\circ$  to  $21^\circ$ . The usual six components of force and moment were measured. Visual tuft studies and motion pictures were made of the action of tufts which were attached to the wing upper surface. These tests were made at a Reynolds number of approximately  $4.1 \times 10^6$ .

#### RESULTS

The jet-boundary effects, the blocking effects, the stream alinement, and the tares caused by the wing support struts were calculated for the zero yaw condition and were used for correcting the angles of attack, the longitudinal-force, the lift, and the pitching-moment coefficients of the data given herein at all angles of yaw. No corrections were applied to the yawing and rolling-moment coefficients. Due to the slight variation of the tunnel speed with angle of attack the results in figure 4 and figure 5 are presented for Reynolds numbers at zero lift and at maximum lift, respectively.

For convenience the discussion is presented in three parts. The first part deals with the scale effect on the aerodynamic

characteristics (figs. 4 and 5), the second part deals with the aerodynamic characteristics in yaw (figs. 6 and 7), and the third part deals with the visual tuft studies (fig. 8).

#### Scale Effect on the Aerodynamic Characteristics at Zero Yaw

The effect of Reynolds number on the aerodynamic characteristics of the wing is shown in figure 4. The lift-curve peaks, the drag, and the pitching-moment coefficients were almost unaffected by variations in Reynolds number. The pitching-moment curves (fig. 4(c)) indicate that the wing will be neutrally stable up to a lift coefficient of approximately 0.3 and above this value to a lift coefficient of approximately 0.5 the longitudinal stability of the wing increased. The increased stability between lift coefficients of 0.3 and 0.5 for the wing is attributed to an outward shift in the spanwise location of the center of pressure on each wing panel. From the lift coefficient of 0.5 to about  $C_{L_{max}}$  the pitching-moment curves indicate a rapid increase in pitching moment in the unstable direction. This increase is attributed to inward shift in the spanwise location of the center of pressure on each wing panel. Tuft observation (fig. 8(a)) indicates that as the lift coefficient is increased from approximately 0.5 to about  $C_{L_{max}}$ , the stall moves progressively toward the center sections of the wing. The pitching-moment curves also indicate that the wing at about  $C_{L_{max}}$  will have a diving tendency. The diving tendency at about  $C_{L_{max}}$  would indicate a loss in the load at the root section. Tuft observation (fig. 8(a)) at this attitude indicates that the air flow becomes spanwise and rough near the center portions of the wing. At angles of attack up to approximately  $8^\circ$  the slope of the lift curve increased with angle of attack. Above this value the slope decreased with angle of attack. The drag of the wing is considered fairly high at high angles of attack when compared with round-leading-edge wings.

To show more clearly the variation of  $C_{L_{max}}$  with Reynolds number, a curve of  $C_{L_{max}}$  against Reynolds number is plotted in figure 5. This curve indicates that variation of the Reynolds number had no appreciable effect on  $C_{L_{max}}$ . This is true both because of the fact that the sharp leading edge fixes the point of initial separation, and also because in general the scale effect on  $C_{L_{max}}$  is small on highly swept-back wings (reference 1). Discounting irregularities at the lowest Reynolds numbers, the maximum value of the lift coefficient obtained was 0.87. It will be noticed that a maximum lift point is given in figure 5 at a Reynolds number of  $8.0 \times 10^6$  and no corresponding data are given in figure 4. The results for a Reynolds number of  $8.0 \times 10^6$  were substantially identical to those for a Reynolds number of  $6.8 \times 10^6$ .

### Aerodynamic Characteristics in Yaw

The aerodynamic characteristics of the wing over a range of yaw angle at several angles of attack are presented in figure 6. The lateral stability parameters  $C_{l\psi}$ ,  $C_{n\psi}$ , and  $C_{y\psi}$  of the wing are plotted in figure 7 as a function of lift coefficient. The slopes of  $C_{l\psi}$ ,  $C_{n\psi}$  and  $C_{y\psi}$  were taken from the curves similar to those of figure 6(a) at  $0^\circ$  angle of yaw and are therefore appropriate to the values of lift coefficient for  $0^\circ$  yaw. At lift coefficients up to 0.4 the rolling moment increased nearly linearly with yaw in the direction to raise the forward wing panel. Above this value the rolling moments change irregularly in the direction to lower the forward wing panel. This variation of rolling moment with yaw indicates that the forward wing panel stalled first. Tuft observations (fig. 8(b)) also indicate the same results.

At a lift coefficient up to 0.3 the yawing moment of the wing changes very little with yaw. Above this value the yawing moments change fairly slowly and irregularly with yaw.

The effective dihedral parameter  $C_{l\psi}$  increased with lift coefficient up to a lift coefficient of 0.1. At lift coefficient of 0.1 the maximum value of  $C_{l\psi}$  of 0.0004 corresponding to  $2^\circ$  of geometric dihedral was obtained and  $C_{l\psi}$  remained approximately constant from  $C_L = 0.1$  to  $C_L = 0.38$ . The value of  $C_{l\psi}$  then decreased and finally reversed in sign at a lift coefficient of 0.45, that is, a negative dihedral effect was obtained. The maximum value of  $C_{l\psi}$  of the wing is considered very small when compared with the maximum effective dihedral of wings having round leading edges (reference 2).

The directional stability parameter  $C_{n\psi}$  is approximately neutral up to a lift coefficient of 0.45. The maximum value of  $C_{n\psi} = -0.00004$  was obtained at a lift coefficient of 0.26. Above the lift coefficient of 0.45 the value of  $C_{n\psi}$  increased rapidly and unfavorably.

### Tuft Studies

The results of the tuft studies for  $0^\circ$  and  $3.7^\circ$  yaw are presented in figure 8.

At zero yaw and low angles of attack the air flow over the wing is similar to that for a swept-back wing having conventional airfoil

sections. At an angle of attack of about  $5.5^\circ$  there begins a spanwise air flow toward the wing tips starting at about 30 percent of the semispan of the wing which causes tip stall. As the angle of attack is increased the stalled region moves progressively toward the root.

The tuft studies at an angle of yaw of  $3.7^\circ$  (fig. 8(b)) indicate that the forward wing panel starts to stall at a lower angle of attack than the retarded wing panel. For angles of yaw greater than  $3.7^\circ$  the tuft studies indicate that the stall angle of attack for the forward wing panel is decreased as the angle of yaw is further increased. For the higher angles of yaw ( $9.9^\circ$ ,  $15^\circ$ , and  $20.8^\circ$ ) the forward wing panel is completely stalled at high angles of attack, whereas the flow on the retarded wing panel remains orderly.

#### DISCUSSION OF FLOW PHENOMENA

The results obtained with this wing are somewhat contradictory to those that have been obtained with swept-back wings having conventional airfoil sections. It is, therefore, desirable to take note of some of the flow phenomena that produce these results, especially since they are believed to be characteristic of highly swept-back wings having airfoil sections with sharp leading edges. A difference between the flow over wings of this type and wings having conventional airfoil sections with round leading edges is to be expected inasmuch as the flow over the basic airfoil sections themselves is also quite different. Consider first the flow over the basic airfoil in two dimensions. The sharp-leading-edge airfoil is characterized by a very early separation at the leading edge and the formation of a so-called bubble of separation, aft of which the flow reestablishes itself and continues in a more or less normal fashion; whereas, a conventional section which is characterized by an initial separation occurs at a much higher angle of attack and further aft on the airfoil surface.

When the sharp-leading-edge wing is swept back, the flow tries to separate at the leading edge at a low angle of attack (in the case of this wing about  $5\frac{1}{2}^\circ$  or at a  $C_L$  of about 0.3). On account of the relief in the adverse pressure gradient that results from high sweepback, however, the air simply flows spanwise at the leading edge. These effects are indicated in the tuft surveys of figure 8(a). The spanwise flow at the leading edge contributes greatly toward the early stalling of the tip, which stalls first at the leading edge due to the combined effects of the spanwise flow and of the

sharp leading edge. On swept-back wings with conventional airfoil sections, by contrast, the stall ordinarily has been observed to start at the trailing edge of the tip because of outward flow of the boundary layer on the after portions of the wing.

When a swept wing sideslips, the effect is similar to that which would be created by decreasing the sweep of the leading wing and increasing the sweep of the trailing wing. Contrary to the results obtained with wings of conventional airfoil sections, decreasing the sweep of the biconvex wing does not alleviate the stall appreciably, and in fact in some sweep ranges may, as in this case, even aggravate it. Likewise, increasing the sweep of the biconvex wing may improve the flow conditions by a flow mechanism similar to the large vortex observed on the DM-1 glider after the sharp leading edges were added (reference 3). The generally low effective dihedral of this wing and the early change from positive to negative effective dihedral then appears to result from the combined effects of these changes in the flow due to the sideslip and the early tip stall. The tuft surveys of figure 8 show these effects quite clearly. Although high effective dihedral has been one of the most serious problems confronting the designer attempting to use swept-back wings, the low effective dihedral of this wing is by no means considered a solution to the problem, because it would probably be almost impossible to maintain adequate lateral control by conventional methods after the tip had begun to stall and because of the longitudinal instability experienced at moderate and high angles of attack. These problems do not appear to be unsolvable, but further experimental investigation and study of the fundamental-flow phenomena will be required before they can be successfully overcome.

#### SUMMARY OF RESULTS

The results of force tests of a  $45^\circ$  swept-back wing having biconvex airfoil sections in the Langley full-scale tunnel are summarized as follows:

1. From low-speed considerations, the wing has poor characteristics which are primarily due to early tip stallings.
2. The maximum lift coefficient obtained for the wing is 0.87.
3. The wing is neutrally stable up to a lift coefficient of approximately 0.3 and above this value to a lift coefficient of approximately 0.5 the longitudinal stability of the wing increases,

however, above a lift coefficient of 0.5 to about maximum lift coefficient the wing is longitudinally unstable.

4. The wing has high drag at high angles of attack.

5. The wing has small positive effective dihedral up to a lift coefficient of 0.45 and above this value the effective dihedral of the wing is negative.

6. The wing has neutral directional stability up to a lift coefficient of 0.45 and above this value the wing becomes directionally unstable.

7. The lift, the drag, and the pitching-moment coefficients are almost unaffected by variations in Reynolds number.

Langley Memorial Aeronautical Laboratory  
National Advisory Committee for Aeronautics  
Langley Field, Va.

#### REFERENCES

1. Sweberg, Harold H., and Lange, Roy H.: Summary of Available Data Relating to Reynolds Number Effects on the Maximum Lift Coefficients of Swept-Back Wings. NACA RM No. L6L20a, 1946.
2. Letko, William, and Goodman, Alex: Preliminary Wind-Tunnel Investigation at Low-Speed of Stability and Control Characteristics of Swept-Back Wings. NACA TN No. 1046, 1946.
3. Wilson, Herbert A., Jr., and Lovell, J. Calvin: Full-Scale Investigation of the Maximum Lift and Flow Characteristics of an Airplane Having Approximately Triangular Plan Form. NACA RM No. L6K20, 1946.

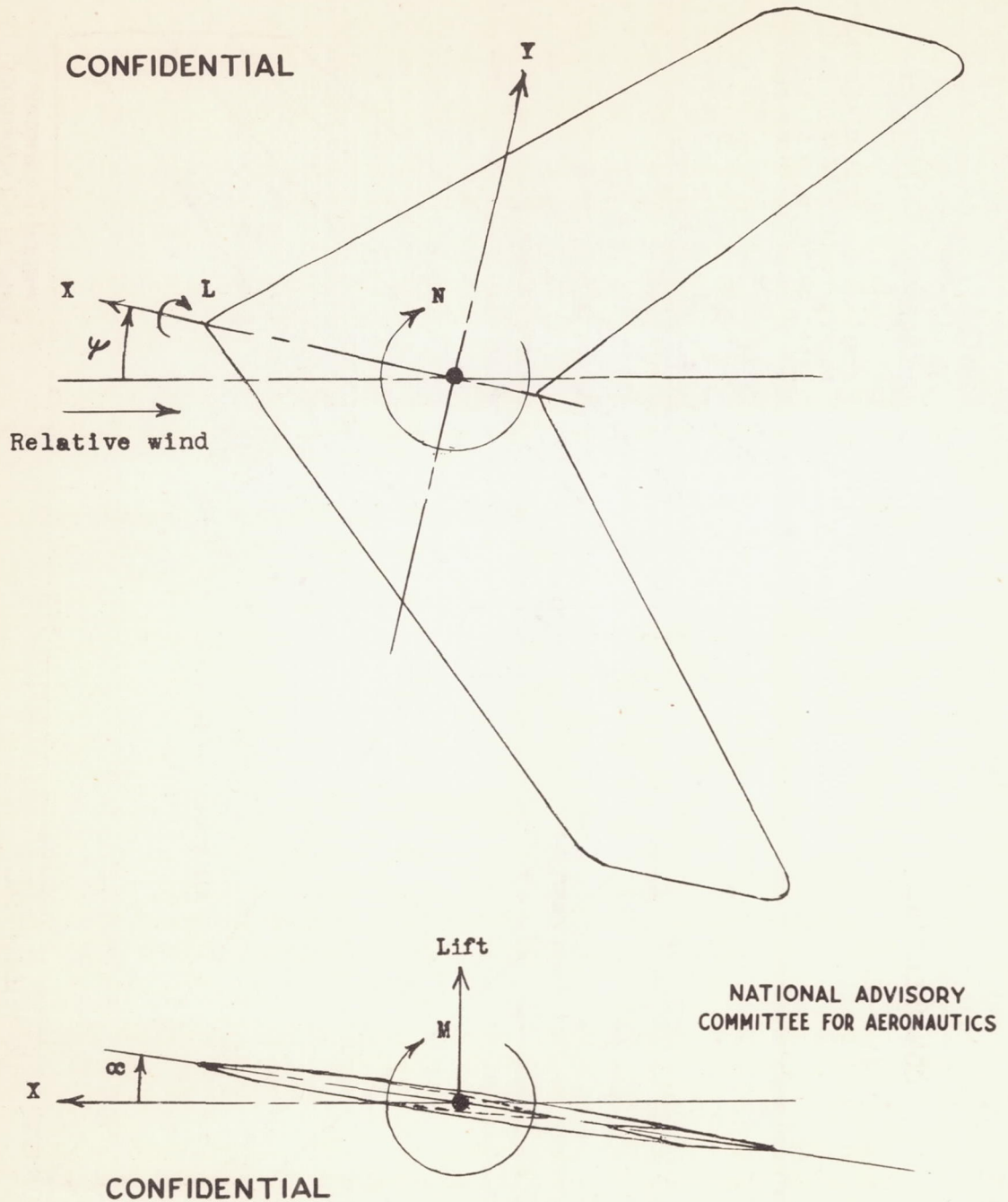


Figure 1.- System of axes. Positive values of forces, moments, and angles are indicated by arrows.

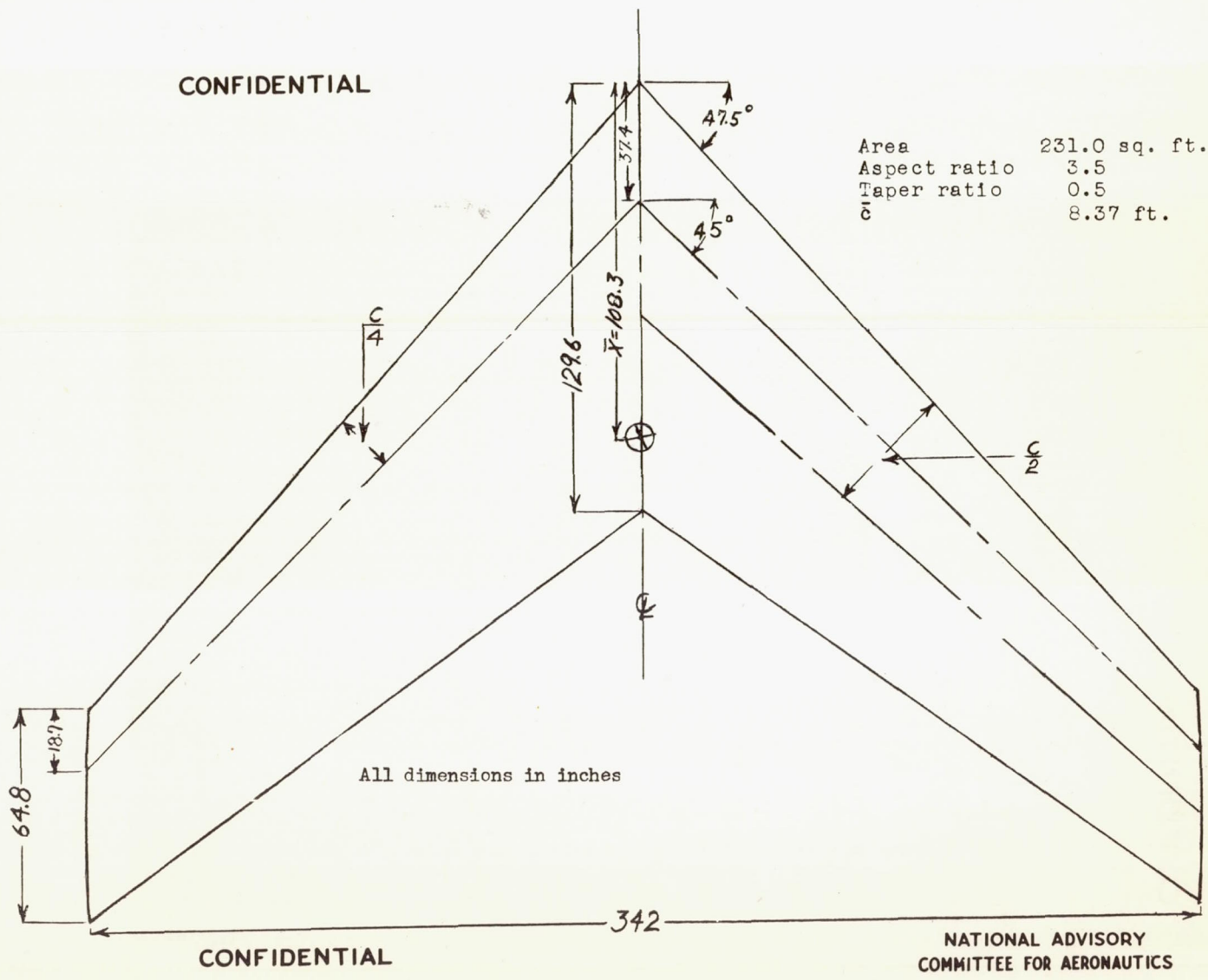


Figure 2.- Plan form of 45° swept-back wing.

CONFIDENTIAL

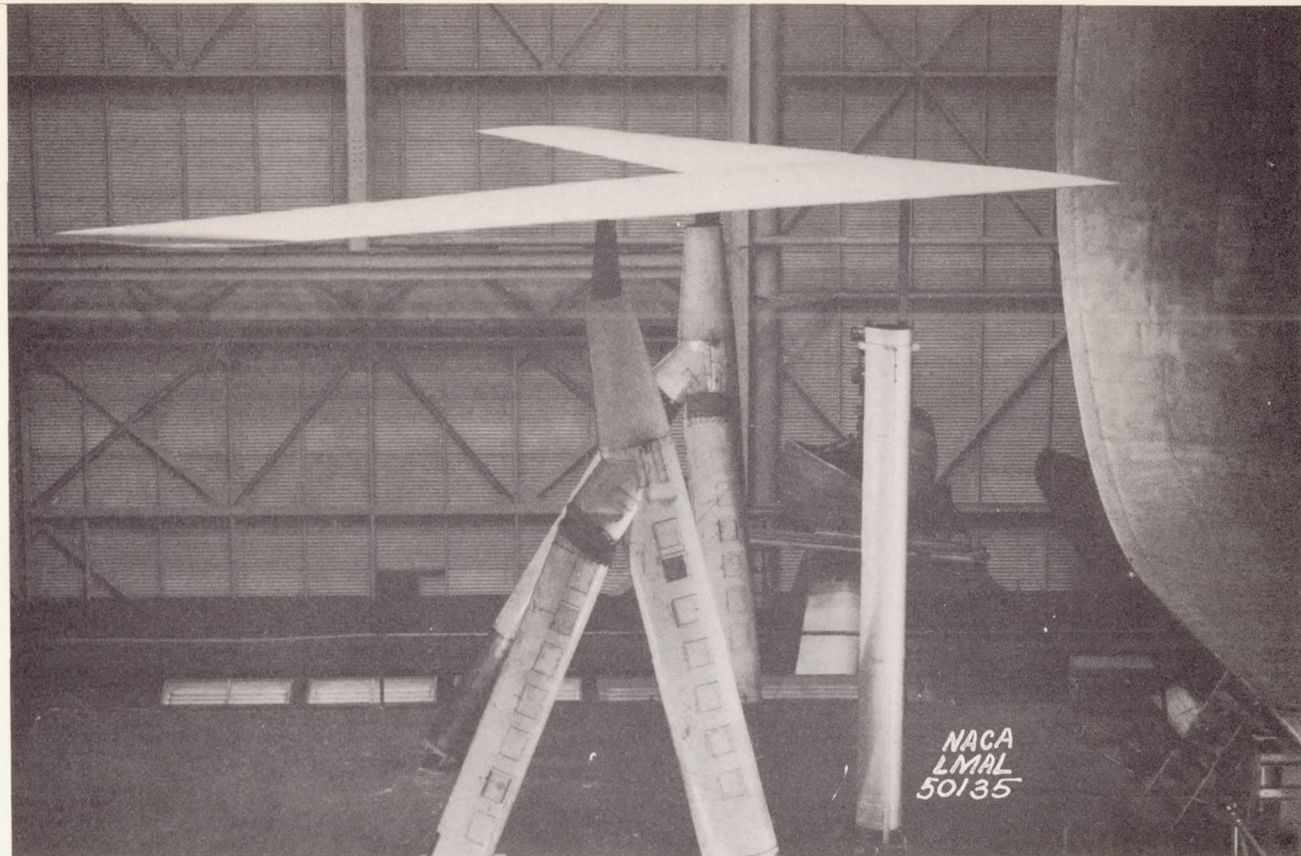
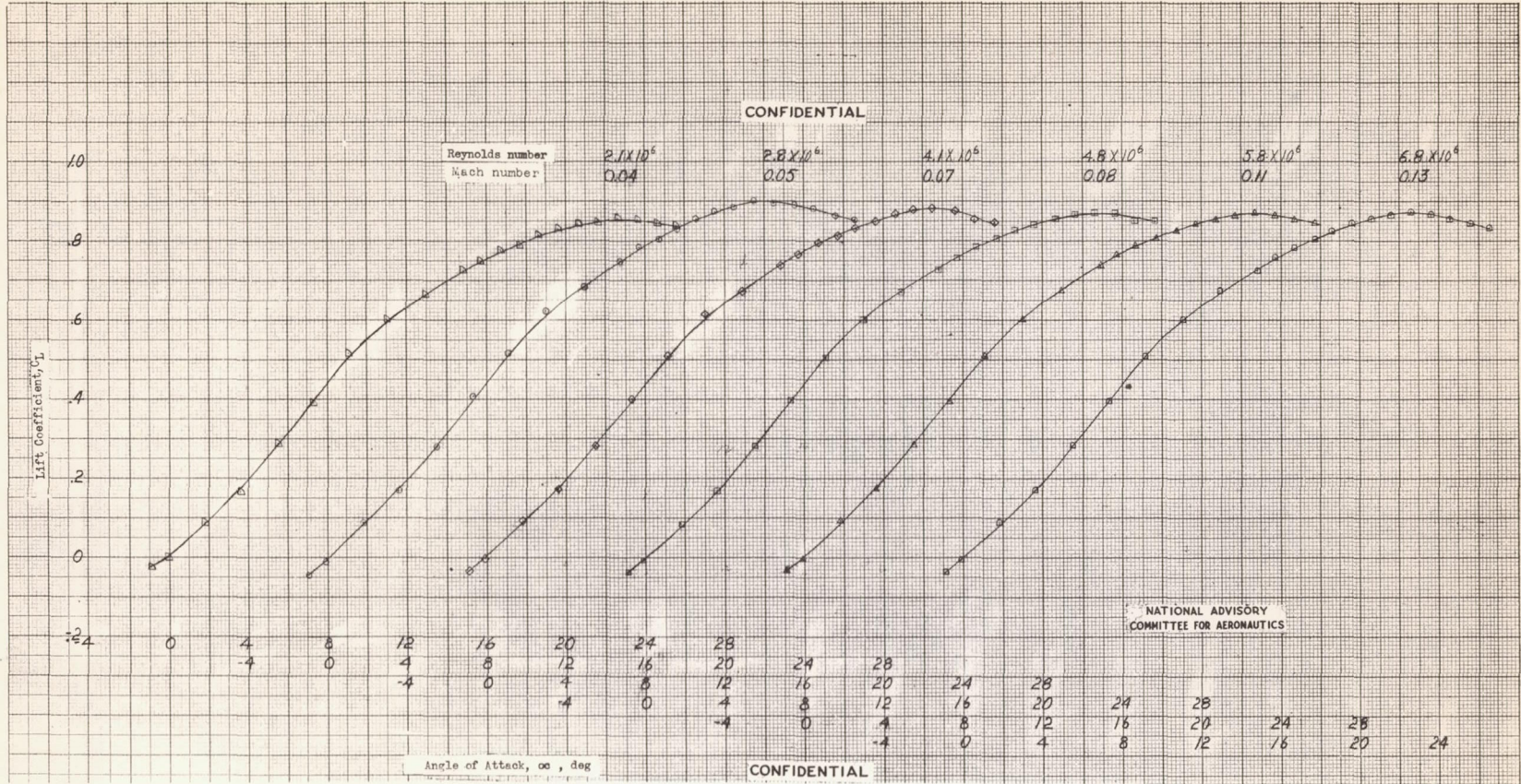


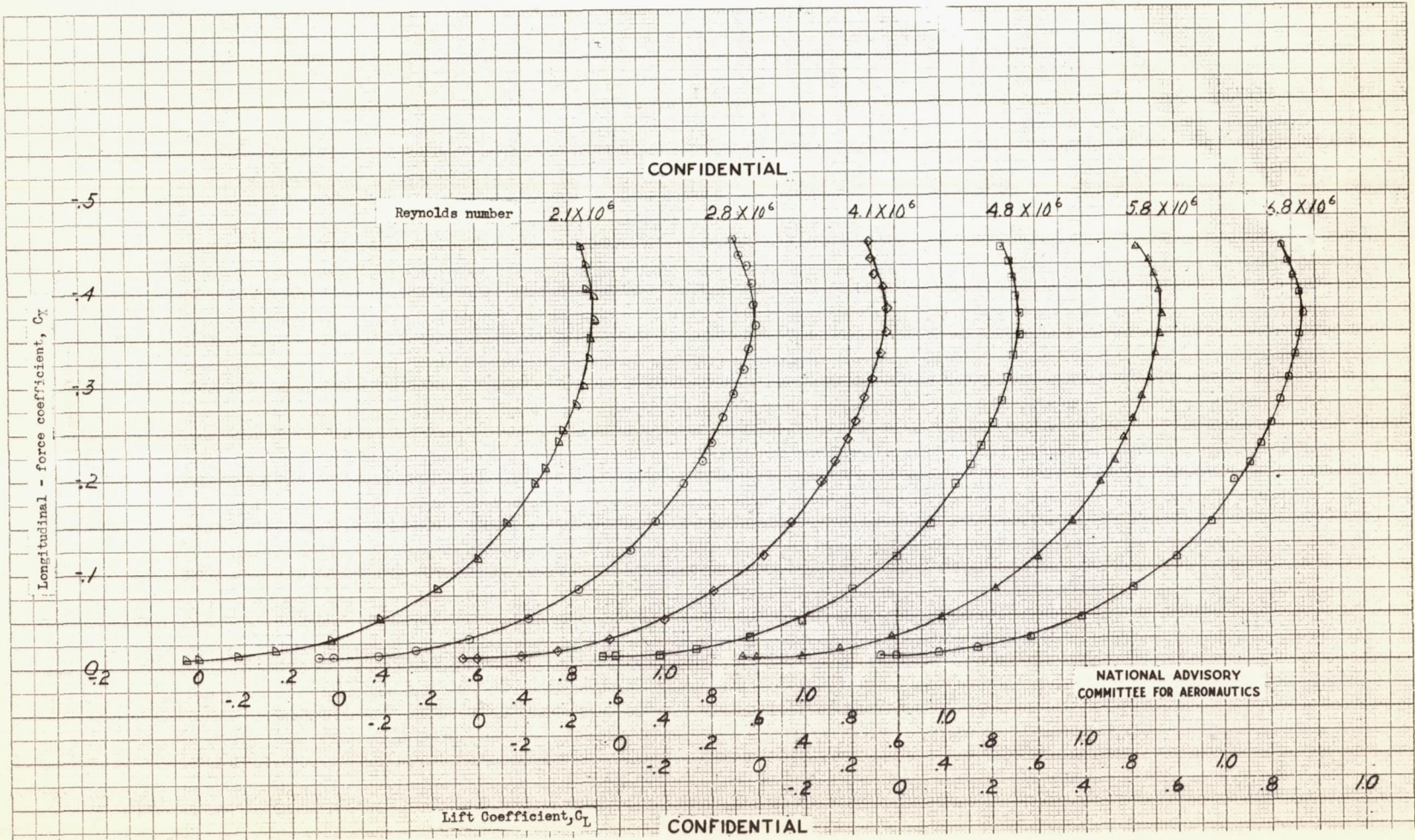
Figure 3.- Side view of  $45^{\circ}$  swept-back wing mounted in the Langley full-scale tunnel.  
 $\psi = +3.7^{\circ}$ .

CONFIDENTIAL



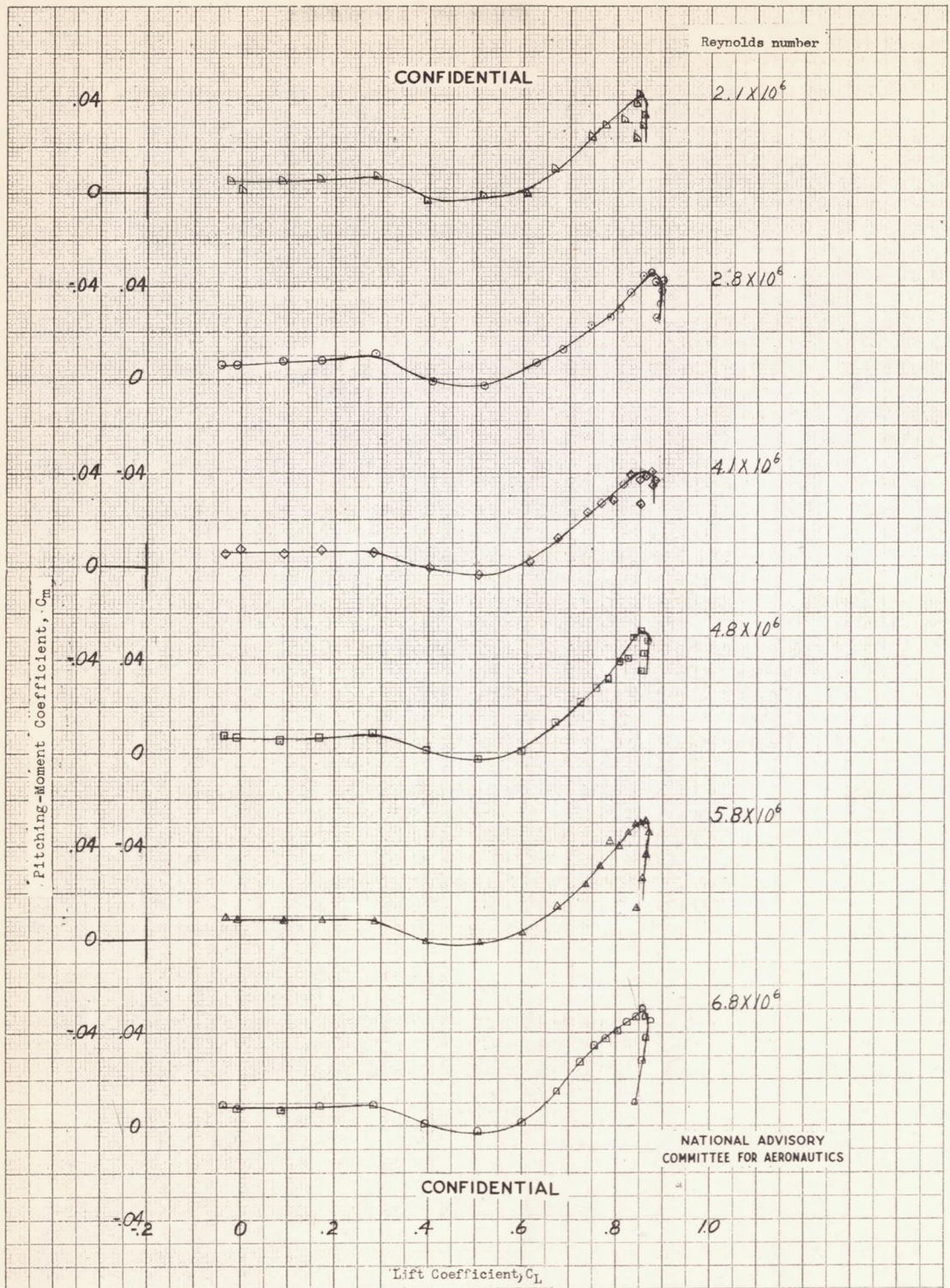
(a)  $C_L$  versus  $\alpha$ .

Figure 4.- Effect of Reynolds number on lift, drag, and pitching-moment coefficients of a  $45^\circ$  swept-back wing.  $A = 3.5$ ;  $\lambda = 0.5$ ;  $\psi = 0^\circ$ .



(b)  $C_x$  versus  $C_L$ .

Figure 4.- Continued.



(c) C<sub>m</sub> versus C<sub>L</sub>.

Figure 4.- Concluded.

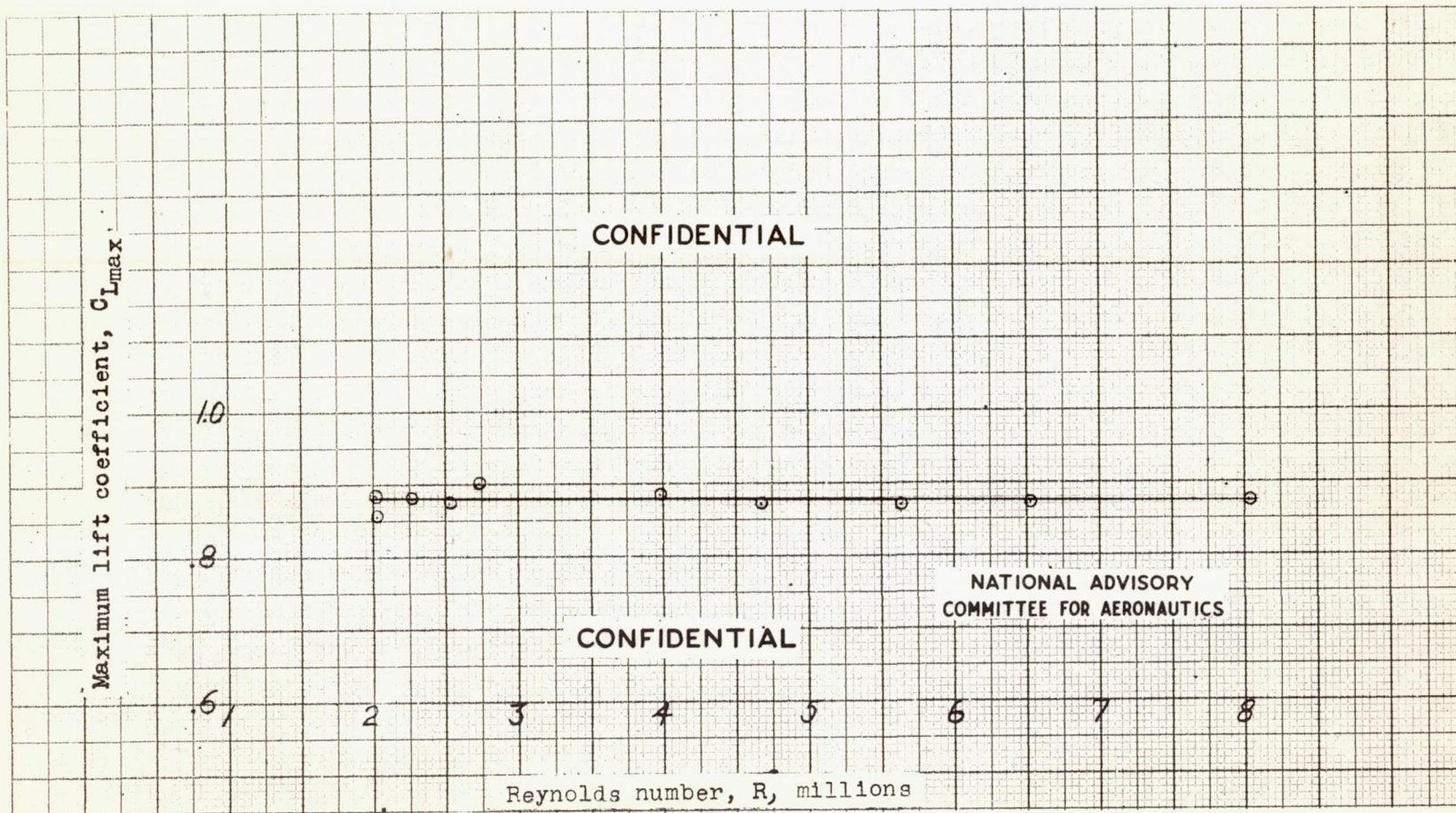
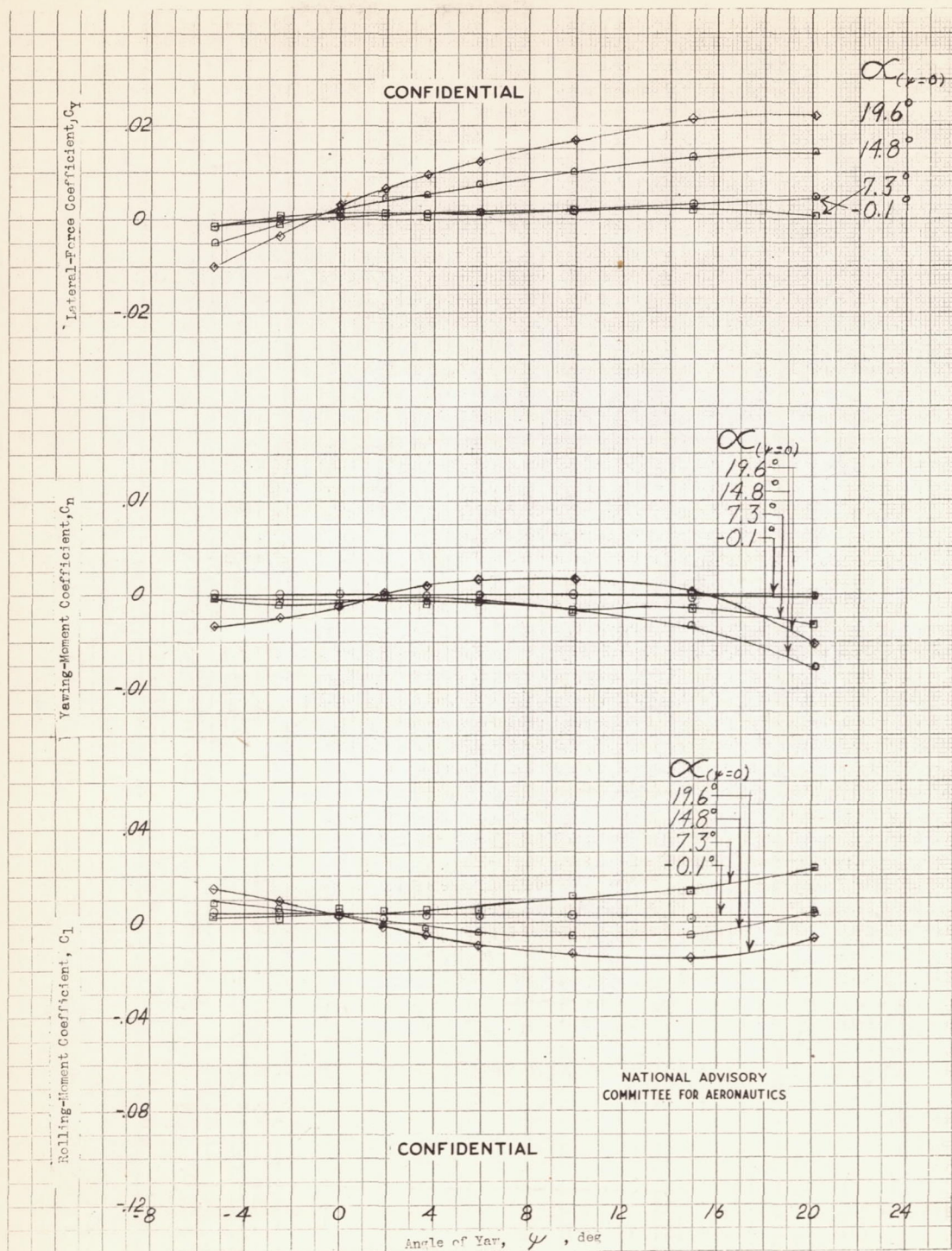
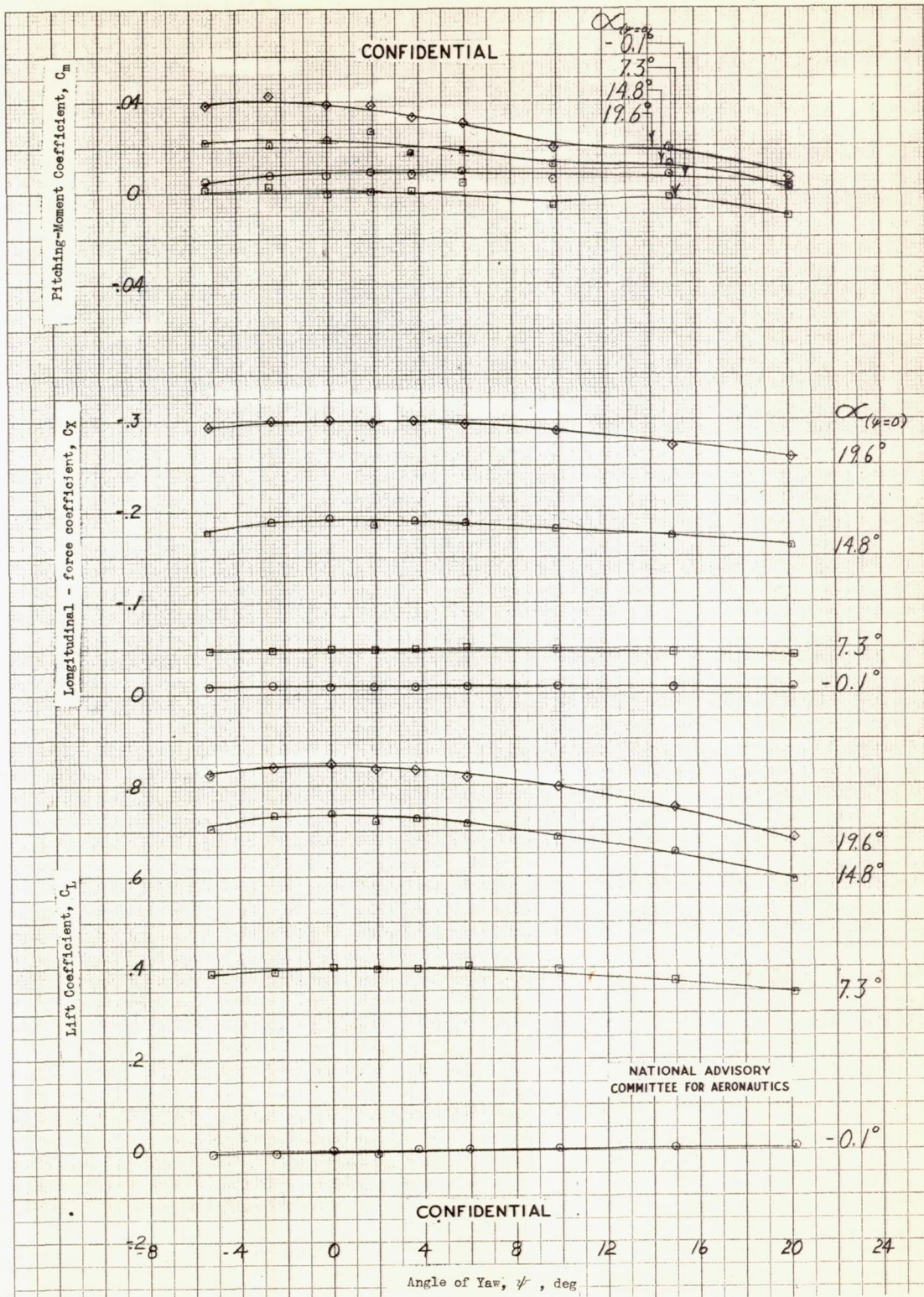


Figure 5.- Effect of Reynolds number on  $C_{L_{max}}$  of a  $45^\circ$  swept-back wing.  $A = 3.5$ ;  $\lambda = 0.5$ ;  $\psi = 0^\circ$ .



(a)  $C_Y$ ,  $C_n$ , and  $C_l$ .

Figure 6.- Variation with angle of yaw of the aerodynamic characteristics of a  $45^\circ$  swept-back wing.  $A = 3.5$ ;  $\lambda = 0.5$ ;  $R = 4.10 \times 10^6$ .



(b)  $C_m$ ,  $C_x$ , and  $C_L$

Figure 6.- Concluded.

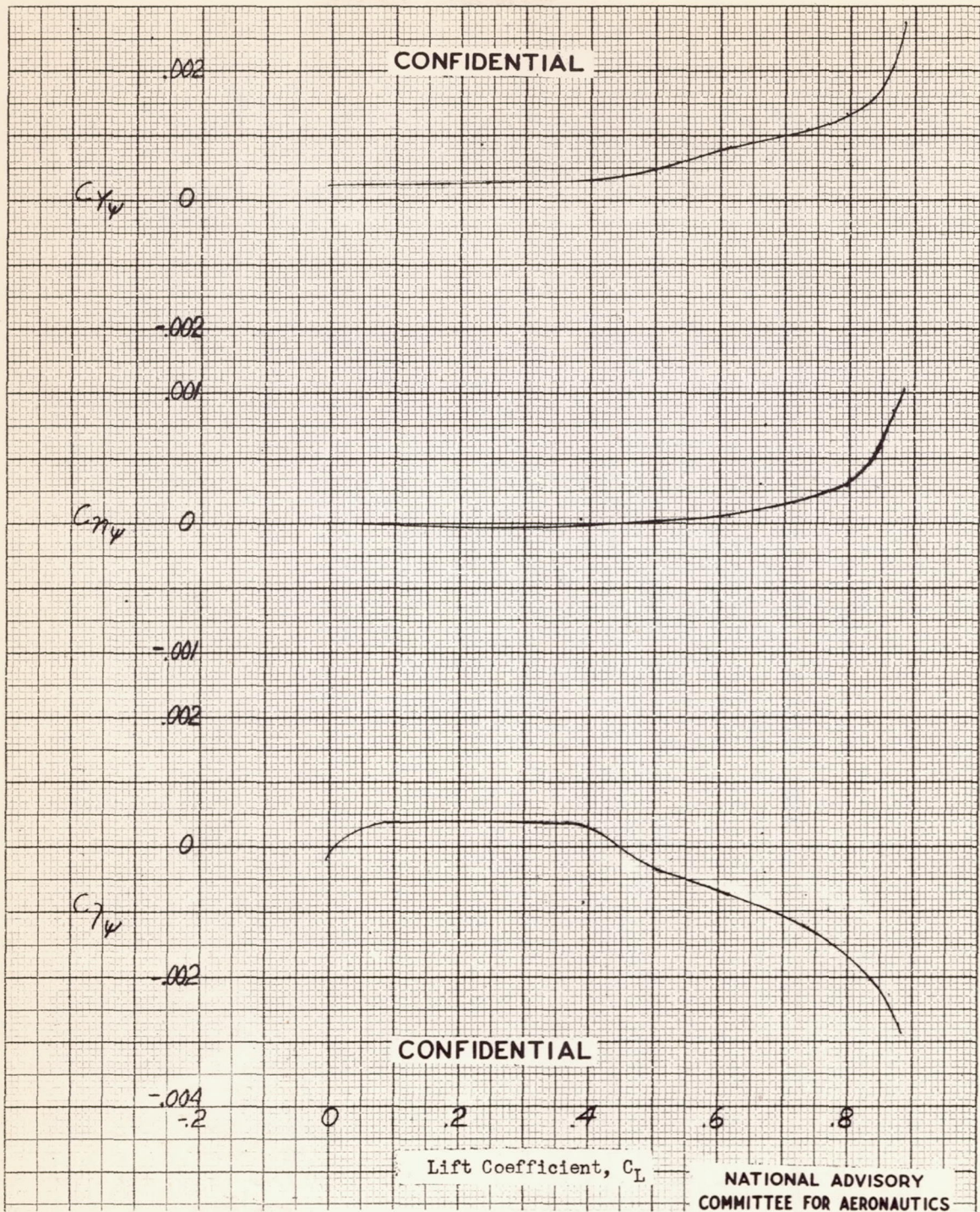
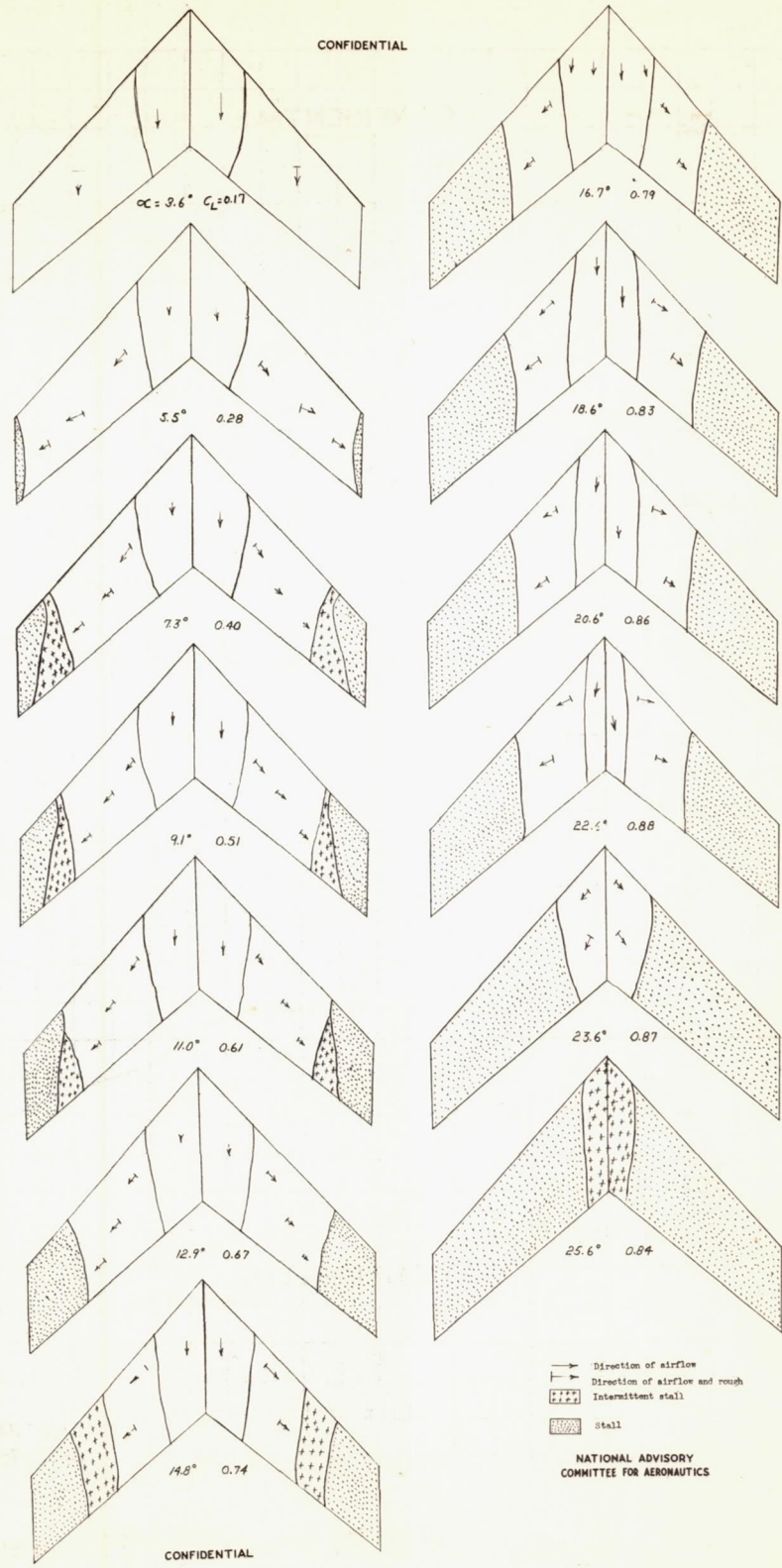
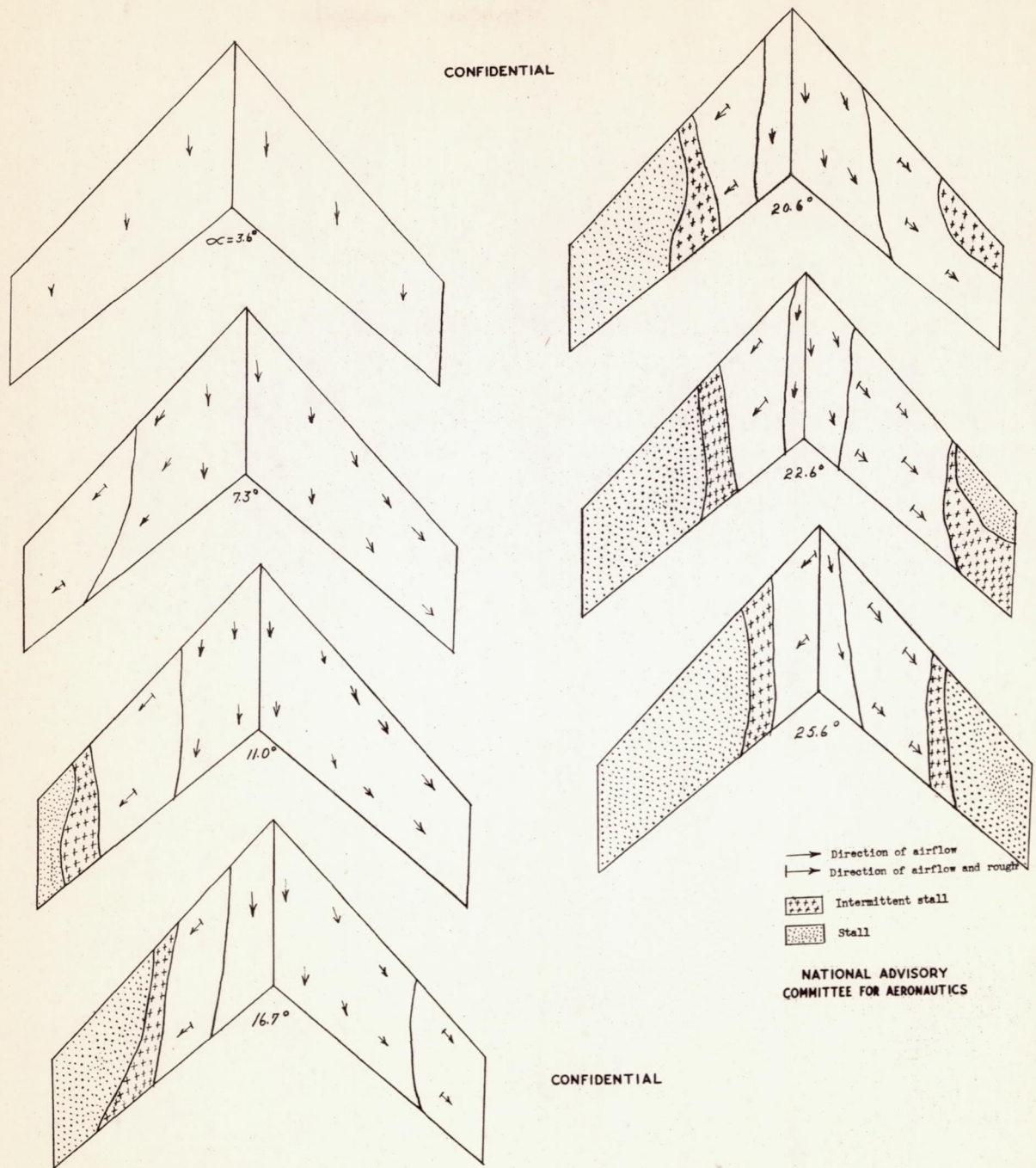


Figure 7.- Lateral stability parameters of a 45° swept-back wing.



(a)  $\psi = 0^\circ$

Figure 8.- Tuft studies for a 45° swept-back wing.  
 $R = 4.10 \times 10^6$ .



(b)  $\psi = +3.7^\circ$ .

Figure 8.- Concluded.